Available online at www.sciencedirect.com

SciVerse ScienceDirect

Ceramics International 39 (2013) 7983–7988

CERAMICS INTERNATIONAL

www.elsevier.com/locate/ceramint

Co-precipitation synthesis and two-step sintering of YAG powders for transparent ceramics

Xianxue Li[a], Bingyun Zheng[a,*], Tareque Odoom-Wubah[b,c], Jiale Huang[b,c,**]

[a]*Department of Environment & Life Sciences, Putian University, Putian, Fujian 351100, PR China*

[b]*Department of Chemical and Biochemical Engineering, College of Chemistry and Chemical Engineering, and National Laboratory for Green Chemical Productions of Alcohols, Ethers and Esters, Xiamen University, Xiamen 361005, PR China*

[c]*Key Lab for Chemical Biology of Fujian Province, Xiamen University, Xiamen 361005, PR China*

Received 29 January 2013; received in revised form 13 March 2013; accepted 18 March 2013
Available online 26 March 2013

Abstract

Yttrium aluminum garnet ($Y_3Al_5O_{12}$, YAG) precursor was synthesized by the co-precipitation method with ammonium hydrogen carbonate as the precipitant. The influence of aging and calcination temperature on the precursor composition and transformation temperature of the YAG phase was investigated. On that basis, a two-step sintering (TSS) method (heating the sample up to 1800 °C followed by holding it at 1600 °C for 8 h) was used to fabricate bulk transparent YAG ceramics in vacuum (10^{-3} Pa) in this communication. A variety of techniques, such as X-ray powder diffraction, infrared spectra, scanning electron microscopy and UV–vis–NIR spectrophotometry were adopted to characterize the resulting YAG powders and ceramics. The results showed that aging had a dramatic effect on the precursor composition, which in turn influenced the transformation temperature of the YAG phase. Loosely agglomerated YAG powders with a mean particle size of 50 nm were obtained by calcinating the precursor without aging at 1000 °C. Finally, a transparent YAG ceramic specimen, achieving the in-line transmittance of 41% in the visible wavelength region and a nearly pore-free microstructure with uniform grains of about 4 μm, was produced via the TSS technique.

Keywords: A. Sintering; YAG; Co-precipitation

1. Introduction

Yttrium aluminum garnet ($Y_3Al_5O_{12}$, YAG) is an advanced structural ceramic material due to its high creep and oxidation resistance at high temperatures [1]. In the last decade, transparent YAG ceramic has become a research focus in the material field because of its several advantages in cost, composition control, scalability and ease of manufacturing [2–4]. Moreover, YAG ceramic can achieve a high neodymium doping concentration and large size samples, which is of great significance for high-power solid-state lasers [5]. Given such prospective application potential, exploring synthesis techniques yielding transparent YAG ceramic becomes highly desirable.

Above all, solid-state reaction method has been a frequently available way for transparent ceramics. In 1995, Ikesue et al. [6] fabricated transparent YAG ceramic by this method using high-purity Al_2O_3 and Y_2O_3 powders with particles smaller than 2 μm as the starting materials. However, the incorporation of some impurities is unavoidable during ball milling, which would in turn influence the transmittance of YAG ceramics. Different from the solid-state reaction, solution-based techniques starting with pre-formed YAG powder rather than oxides via wet-chemical methods, which can achieve better chemical homogeneity through molecular level mixing of the starting materials [7], have recently become a hot research area. Several wet-chemical methods, such as co-precipitation [8–13], combustion synthesis [14–16], sol–gel [17], spray pyrolysis [18], hydrothermal (or solvothermal) synthesis [19,20] and modified citrate process [21], etc., have been extensively investigated in recent years for preparing YAG powders suitable for transparent ceramics. Among these, the

*Corresponding author. Tel.: +86 594 2652865; fax: +86 594 2631931.

**Corresponding author at: Department of Chemical and Biochemical Engineering, College of Chemistry and Chemical Engineering, and National Laboratory for Green Chemical Productions of Alcohols, Ethers and Esters, Xiamen University, Xiamen 361005, PR China. Tel.: +86 594 2652865; fax: +86 594 2631931.

E-mail addresses: zhengybingyun@gmail.com (B. Zheng), cola@xmu.edu.cn (J. Huang).

0272-8842/$ - see front matter © 2012 Elsevier Ltd and Techna Group S.r.l. All rights reserved.
http://dx.doi.org/10.1016/j.ceramint.2013.03.064

co-precipitation method is a relatively convenient and cost-effective way for powder synthesis, and several precipitants, up to now, such as ammonia [22–24] and ammonium hydrogen carbonate (hereafter simply referred to as AHC) [8,13], have been employed to produce YAG powders. However, for ammonia, the pH values of the reaction solutions during the co-precipitation process have to be kept at a constant value ranging from 7.8 to 9 [22–24] due to the amphoteric properties of Al, which make the preparation procedures more complex and unmanageable. In contrast, using AHC as the precipitant can not only avoid the above-mentioned problems, but also have access to acquire less-agglomerated, well-sinterable YAG powders via co-precipitation. Consequently, YAG powders synthesized via AHC co-precipitation technology were preferably used to sinter transparent ceramics. Nevertheless, even starting with preformed YAG powder via AHC co-precipitation technology, prolonged sintering at quite high temperatures, generally 1730–1790 °C [2,13], is necessary. On one hand, long soaking time usually results in abnormal grain growth, which in turn frequently causes entrapment of pores within the grains. On the other hand, long soaking time at a high temperature inevitably leads to large energy wastage. Therefore, a sintering schedule should be innovated. In recent years, the two-step sintering (TSS) system, first proposed by Chen and Wang [25], was conduced by heating the sample to a higher temperature then cooling it down and maintaining at a lower temperature till full densification was achieved. Such a sintering system has proved effective to avoid abnormal grain growth, facilitating the acquiring of transparent ceramics with pore-free structure and uniform grains [26,27].

In the present work, a TSS technique was introduced to sinter transparent YAG ceramics via powders synthesized by the co-precipitation method with AHC as the precipitant. The details about the synthesis, characterization of YAG powder and its TSS process carried out in this laboratory have been reported in this communique.

2. Experimental

$Y(NO_3)_3 \cdot 6H_2O$ (> 99.9% purity), $Al(NO_3)_3 \cdot 9H_2O$ (> 99.9% purity) and AHC (analytical grade) were used as raw materials for the synthesis of the YAG powders. First, concentrated solutions were obtained by dissolving $Y(NO_3)_3 \cdot 6H_2O$ and $Al(NO_3)_3 \cdot 9H_2O$ in distilled water, and Y^{3+} and Al^{3+} concentrations of the nitrate solutions were assayed by the inductively coupled plasma (ICP) spectrophotometric technique. Next, mixed solutions of $Y(NO_3)_3$ and $Al(NO_3)_3$, prepared from the above concentrated salt solutions with appropriate volume to maintain the Y:Al molar ratio at 3:5, were dripped into a 1.5 mol/L AHC solution under mild stirring at 50 °C. Finally, the resultant precursor precipitate was filtered, washed, dried at 60 °C for 1 day, and calcinated at various temperatures for 2 h to obtain YAG powders. To examine the effects of aging on precursor property, the as-prepared precipitate was specially aged for 6 h under mild stirring in order to distinguish them from the precursor without aging.

The YAG powders thus obtained were ball milled with a solvent, binder and 0.5 wt% sintering aid tetraethoxysilane for 12 h. The milled slurry was dried, sieved, and dry-pressed under 10 MPa into Φ20 mm disks and then cold-isostatically pressed under 200 MPa. Pressed specimens were then pre-sintered at 1000 °C for 10 h in air to remove any residual organics introduced during the molding operation. Finally, the powder compacts were sintered in a molybdenum wire-heated vacuum furnace via the so-called TSS schedule, which was defined as follows: the compacts were first heated to a higher temperature (1800 °C) without soaking time, then immediately cooled down and held at a lower temperature (1600 °C) for 8 h (such a TSS schedule was denoted thereafter as 1800 °C × 0 h+1600 °C × 8 h). During the sintering period, the vacuum degree was 10^{-3} Pa. After sintering, the specimens were annealed at 1450 °C for 6 h in air. To compare with the TSS method, two single-step sintered reference ceramic samples were also derived with the same as-synthesized YAG powders at temperatures of 1800 °C and 1600 °C in vacuum (10^{-3} Pa). In the single-step sintering running at temperature 1800 °C, the samples were rapidly heated to 1800 °C and immediately cooled down to room temperature. In the single-step sintering running at temperature 1600 °C, the samples were heated to 1600 °C and held at 1600 °C for 8 h.

The crystalline development of the precursor heat-treated at different temperatures was identified by X-ray diffraction (XRD) in a MAC Science MXP21VAHF diffractometer. Infrared (IR) spectra were recorded employing a Bruker (TENSOR-27) FT-IR spectrometer by a KBr disk method. Morphologies of the resultant YAG powders and microstructures of the sintered ceramic specimens were examined using scanning electron microscopy (SEM) (Model S-4300, Hitachi, Tokyo, Japan). For sintered bodies, the surface of the sample was polished to 1 mm finish with diamond paste and thermally etched at 1500 °C for 2 h to reveal the grain boundaries. Fracture surfaces of the specimens were also observed using SEM. Sintered density was measured by the Archimedes method, using deionized water as the immersion medium. Transmittance of the mirror-polished sample on both surfaces was measured using a Lambda-900 UV–vis–NIR spectrophotometer at room temperature.

3. Results and discussion

3.1. Powder properties

The XRD spectra of the precursor without aging and its calcined products at various calcination temperatures are shown in Fig. 1. Obviously, the as-prepared precursor without aging is amorphous. As the calcination temperature increases to 800 °C, crystallization starts to occur. At 900 °C, the XRD pattern of the as-prepared powders matches well with the YAG cubic crystal structure (ICSD Card no. 20090), without detecting any intermediate impurity phases. When calcinated at 1000 °C, no change in phase composition is found while the diffraction peaks become narrower and higher than those obtained at 900 °C, which are attributed to the increase of crystallite size and improved crystallinity at the higher heating temperature. Besides, to examine the effect of aging on precursor property, Fig. 2 presents the XRD pattern of the precursor aged for 6 h and its calcined products at various calcination temperatures. As shown, many small diffraction peaks appear in the XRD pattern of this precursor, indicating

that the precursor composition changes during the aging period. More strangely, this aging process, on the contrary, leads to the emergence of intermediate impurity phases, namely, $Y_4Al_2O_9$ (YAM) and $YAlO_3$ (YAP), which, however, cannot be found during the calcination process for the precursor without aging. As shown, when the calcination temperature increases from 900 °C to 1200 °C, YAM and YAP, in addition to the YAG phase, are detected. Nevertheless, at 1300 °C, pure YAG with cubic crystal structure (ICSD Card no. 20090) is exactly available, suggesting that the aging for 6 h has already caused the very high transformation temperature needed to produce pure YAG powder from this precursor. The reason for this lays possibly in the fact that there was an exchange of CO_2 and water between the precursor solution and air during the aging process. Dissolution of CO_2 into the solution leads to the reduction of pH value and the evaporation of water into air will change the concentration of ion species, both of which alternate the local chemical environment to which the precursors are exposed. As a result, ions on the precursor surfaces happen to rearrange, which alternatively leads to the composition variation and, therefore, to the inevitable composition segregation in the precursor. Hence, one would expect that the calcination performance of the precursor aged for 6 h is different from that of the precursor without aging.

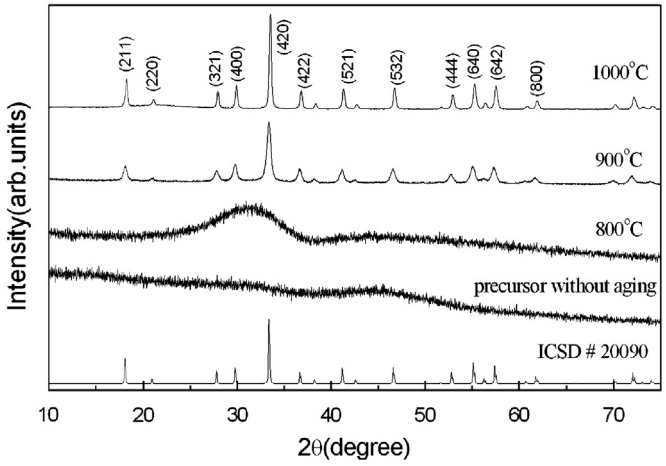

Fig. 1. XRD spectra of the precursor without aging and its calcined products at various calcination temperatures.

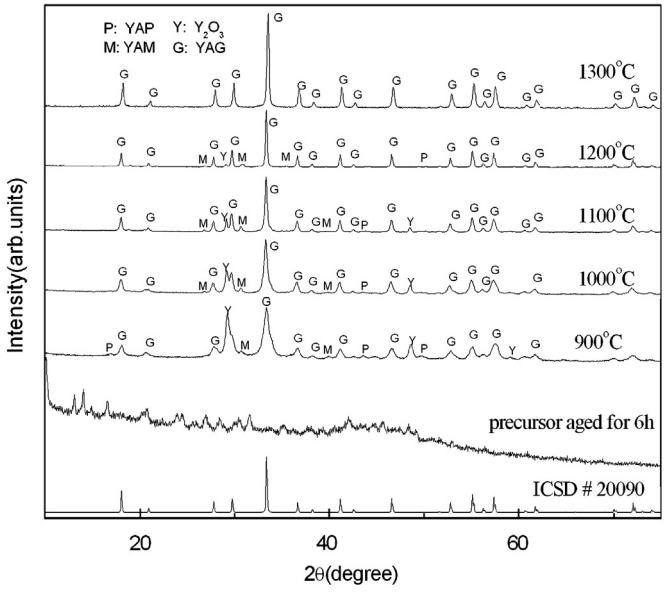

Fig. 2. XRD pattern of the precursor aged for 6 h and its calcined products at various calcination temperatures.

To further reveal the crystallization process, IR spectra of the original precursor without aging and the powders heated at various temperatures were carried out as shown in Fig. 3. The broad absorption band peak at 3450 cm^{-1} is associated with the stretching vibrations of the hydroxyl groups (O–H). Characteristic of H–O–H bending mode of molecular water corresponds to the small band at ~1630 cm^{-1}. Besides, two major peaks, located at ~1385 cm^{-1} and 1518 cm^{-1}, may have resulted from the diagnosis of CO_3^{2-}. As the calcination temperature increases from 800 °C to 900 °C, these double absorption peaks corresponding to CO_3^{2-} gradually weaken and eventually disappear at 900 °C, implying the termination of the decomposition process of CO_3^{2-}. In addition, at 900 °C or above, the metal–oxygen vibration characteristics of Al–O, Y–O, and Y–O–Al stretches are clearly observed in the range of ~400–800 cm^{-1}, confirming the formation of a pure YAG phase, which is in good agreement with the above XRD results in Fig. 1.

Fig. 4 shows SEM micrographs of the as-synthesized precursor and the YAG powders calcined at different temperatures. As shown, the precursor without aging [Fig. 4a] is composed of extremely fine particles that are difficult to identify by the SEM method. After aging for 6 h, these fine particles [Fig. 4b] appear to grow bigger and an appreciable agglomeration comes into being, which can also be responsible for the above very high transformation temperature needed to produce pure YAG powder in the above XRD results of Fig. 2. Besides, Fig. 4c and d provides the obtained YAG powders by calcinating the as-synthesized precursor without aging at 900 °C and 1000 °C, respectively. Obviously, the observed particles become gradually

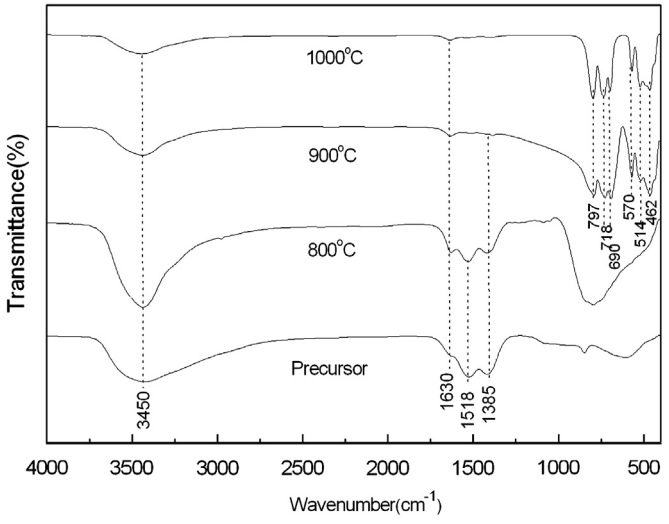

Fig. 3. IR spectra of the precursor without aging and its calcined products at various calcination temperatures.

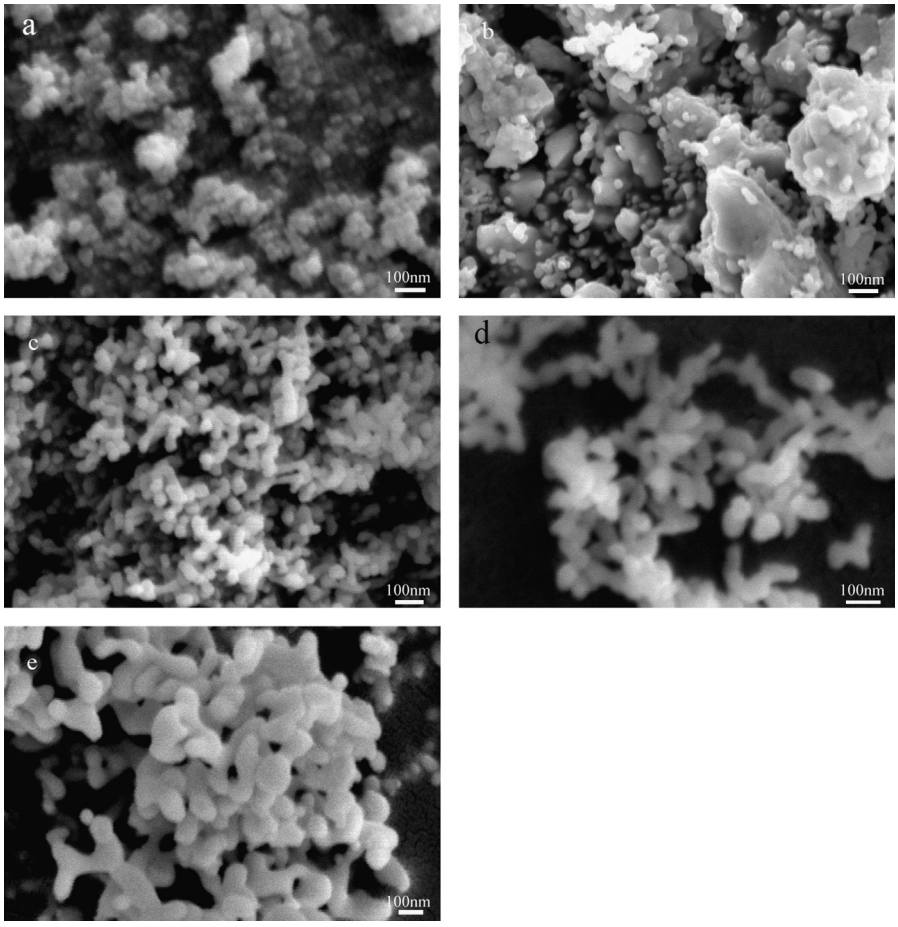

Fig. 4. SEM images corresponding to (a) the precursor without aging; (b) the precursor aged for 6 h; (c) YAG powders by calcinating the precursor without aging at 900 °C; (d) 1000 °C and (e) YAG powders obtained by calcinating the precursor aged for 6 h at 1300 °C.

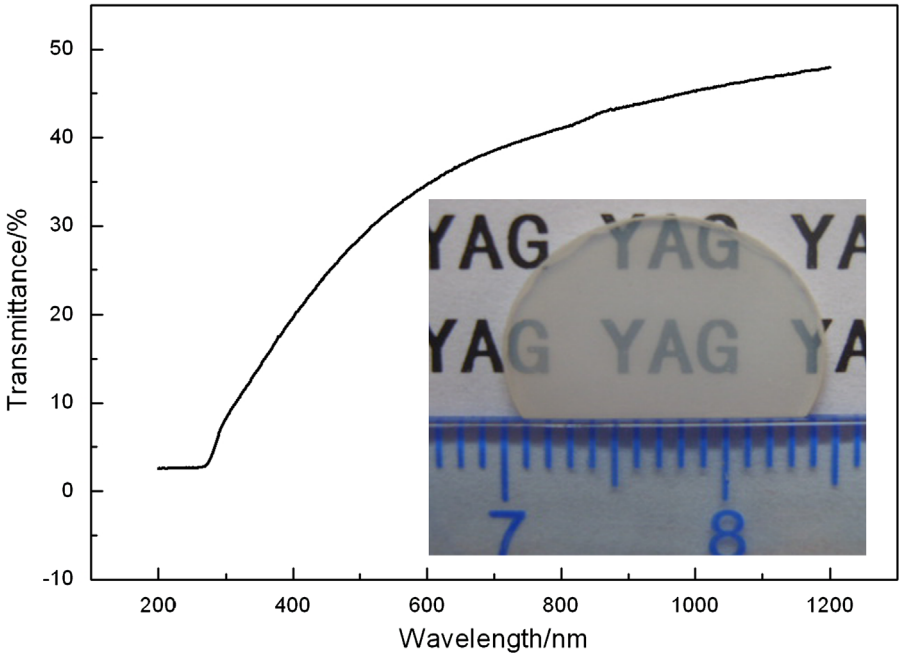

Fig. 5. Light transmission curve and photograph of the mirror-polished YAG sample via TSS method (1800 °C × 0 h+1600 °C × 8 h).

larger with the increase of the calcination temperature, which is in good accordance with the above XRD results shown in Fig. 1. Among them, the observed particles, obtained at 1000 °C, appear to be spherical in shape, agglomerate loosely, and have a particle size of about 50 nm. For comparison, Fig. 4e presents SEM micrograph of the YAG powders produced by calcinating the as-synthesized precursor aged for 6 h at 1300 °C. It can be seen that severe agglomeration, caused by high calcination temperature of 1300 °C, occurs among YAG particles. Such severe agglomeration, however, would in turn result in poor sinterability of the YAG powders for transparent ceramics. Hence, taking the above XRD and SEM results into account, to obtain optimal sintering properties, the YAG powders, derived by heating the precursor without aging at 1000 °C, were therefore chosen to sinter the bulk ceramics thereafter.

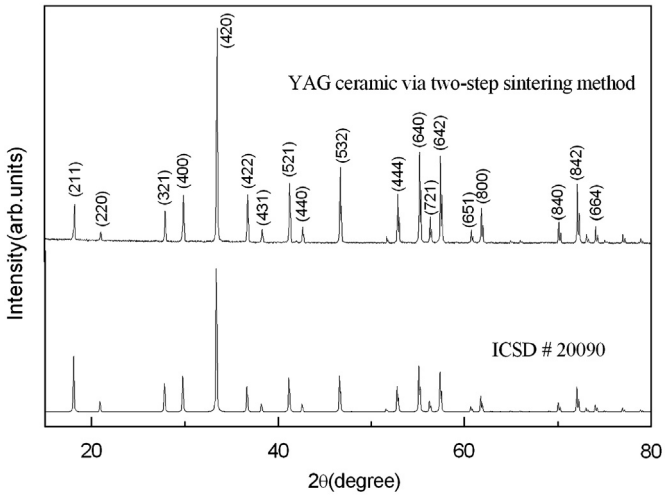

Fig. 6. XRD pattern of the YAG transparent ceramic via TSS method (1800 °C × 0 h+1600 °C × 8 h).

3.2. Ceramic properties

Fig. 5 (inset) shows a photograph of the two-step sintered YAG pellet, which is around 15 mm in diameter and 1.2 mm in thickness with a relative density of about 99.9% of the theoretical value (4.55 g/cm^3). It can be distinctly seen that this ceramic specimen, achieved in-line transmittance of 20–41% in the visible wavelength region (~400–780 nm) as presented in Fig. 5, exhibits good transparency, and the letters can clearly be read through the ceramic. The XRD spectrum of this ceramic sample is also shown in Fig. 6. Distinctly, the XRD pattern agrees well with that of the YAG crystal structure (ICSD Card no. 20090), indicating that there should be no evident second phase in the body of the YAG transparent ceramic. As far as the single-step sintered reference ceramic samples obtained at 1800 °C and 1600 °C are concerned, their relative densities reaches 98.2% and 97.1%, respectively; transparency, however, could not be achieved. Meanwhile, for further comparison, Fig. 7 presents microstructures of the fractured surfaces of these obtained ceramic specimens. As observed in Fig. 7a, the specimen via TSS schedule, possessing a dense and nearly pore-free microstructure, consists of uniform grains (about 4 μm) and no abnormal grain growth is found. However, for the reference ceramic specimens via single-step sintering at 1800 °C and 1600 °C, as shown in Fig. 7b and c, respectively, several obvious pores are detected. Also, the microstructure of the reference ceramic specimen via single-step sintering at 1600 °C is somewhat loose. Hence, we can say that, when the two steps were conducted in succession, the density of the sample is higher than that in the single-step sintering run. Moreover, abnormal grain

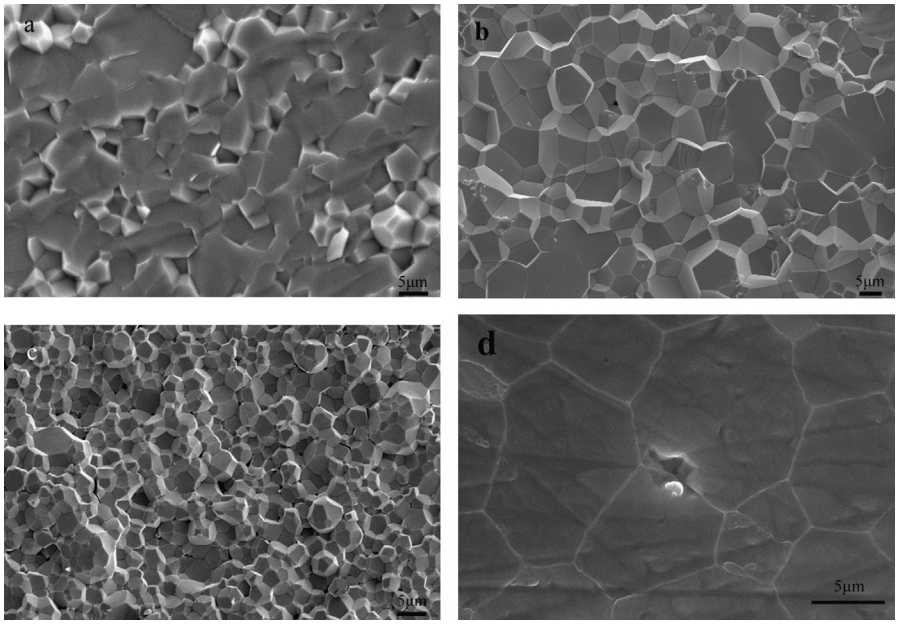

Fig. 7. SEM micrographs of the fractured surfaces of the ceramics sintered by (a) TSS method (1800 °C × 0 h+1600 °C × 8 h); (b) single-step sintering at 1800 °C for 0 h ; (c) single-step sintering at 1600 °C for 8 h; and (d) SEM microstructure of the polished surfaces of the YAG ceramic sintered by single-step sintering at 1800 °C for 0 h.

growth usually resulting from prolonged sintering at 1730–1790 °C can be restrained. The possible interpretation is that, according to the TSS method, at a temperature of 1800 °C, a sufficiently high starting density is reached and all pores in the YAG become subcritical and unstable against shrinkage (as shown in Fig. 7d). Meanwhile, continuous framework forms among the YAG grains, which can serve as an atom diffusion path driving the subsequent sintering step. As we know the activation energy for the grain-boundary diffusion is far lower than that for grain-boundary migration, thus, the energy obtained at temperature 1800 °C is high enough for the grain-boundary diffusion during the subsequent holding process at temperature 1600 °C. Accordingly, the second sintering step at 1600 °C for 8 h can fully promote grain-boundary diffusion through the continuous framework while effectively suppressing grain-boundary migration till full densification is achieved, without forming any obvious pores and abnormal grain growth, just as proposed by Chen and Wang [25]. Relevant experiment optimization via TSS schedule is now being done in order to further improve the transparency of YAG ceramics.

4. Conclusions

The transformation temperature of the YAG phase was influenced by the aging time of the precursor precipitate obtained via AHC co-precipitation method. YAG powders with mean particle size of 50 nm, synthesized by calcinating the precursor without aging at 1000 °C, were densified to good transparency by a TSS technique (heating the sample up to 1800 °C followed by holding at 1600 °C for 8 h) in vacuum condition. The in-line transmittance of the as-obtained YAG ceramic reached 41% in the visible wavelength region, and a dense nearly pore-free microstructure with uniform grains of about 4 μm was achieved. Such a TSS method is anticipated to sinter transparent ceramics more efficiently and economically in the future.

Acknowledgments

The authors acknowledge the financial support from the Natural Science Foundation of China (Grant nos. 21206079, 21106117 and 21036004). The authors would like to thank Dr. Rongqian Yao, Department of Materials Science and Engineering, College of Materials, Xiamen University, for his help with thermal etching of the YAG ceramic samples.

References

[1] X. Zhang, H. Liu, W. He, J. Wang, X. Li, R.I. Boughton, Novel synthesis of YAG by solvothermal method, Journal of Crystal Growth 275 (2005) 1913–1917.
[2] J. Lu, K.-I. Ueda, H. Yagi, T. Yanagitani, Y. Akiyama, A.A. Kaminskii, Neodymium doped yttrium aluminum garnet ($Y_3Al_5O_{12}$) nanocrystalline ceramics-new generation of solid state laser and optical materials, Journal of Alloys and Compounds 341 (2002) 220–225.
[3] A. Ikesue, Y.L. Aung, Synthesis and performance of advanced ceramic lasers, Journal of the American Ceramic Society 89 (2006) 1936–1944.
[4] L. Wang, H. Kou, J. Li, Y. Pan, J. Guo, Preparation of YAG ceramics through a novel process, Ceramics International 38 (2012) 855–859.
[5] A. Ikesue, Polycrystalline Nd:YAG ceramics lasers, Optical Materials 19 (2002) 183–187.
[6] A. Ikesue, I. Furusato, K. Kamata, Fabrication of polycrystal line, transparent YAG ceramics by a solid-state reaction method, Journal of the American Ceramic Society 78 (1995) 225–228.
[7] Y. Wang, L. Zhang, Y. Fan, J. Luo, D.E. McCready, C. Wang, L. An, Synthesis, characterization, and optical properties of pristine and doped yttrium aluminum garnet nanopowders, Journal of the American Ceramic Society 88 (2005) 284–286.
[8] J.-G. Li, T. Ikegami, J.-H. Lee, T. Mori, Y. Yajima, Co-precipitation synthesis and sintering of yttrium aluminum garnet (YAG) powders: the effect of precipitant, Journal of the European Ceramic Society 20 (2000) 2395–2405.
[9] X. Li, W. Wang, Preparation of uniformly dispersed YAG ultrafine powders by co-precipitation method with SDS treatment, Powder Technology 196 (2009) 26–29.
[10] C. Marlot, E. Barraud, S. Le Gallet, M. Eichhorn, F. Bernard, Synthesis of YAG nanopowder by the co-precipitation method: Influence of pH and study of the reaction mechanisms, Journal of Solid State Chemistry 191 (2012) 114–120.
[11] Y. Sang, Y. Lv, H. Qin, X. Zhang, H. Liu, J. Wang, X. Sun, R.I. Boughton, Chemical composition evolution of YAG co-precipitate determined by pH during aging period and its effect on precursor properties, Ceramics International 38 (2011) 1635–1641.
[12] L. Wang, H. Kou, Y. Zeng, J. Li, Y. Pan, J. Guo, Preparation of YAG powders and ceramics through mixed precipitation method, Ceramics International 38 (2012) 4401–4405.
[13] J. Li, F. Chen, W. Liu, W. Zhang, L. Wang, X. Ba, Y. Zhu, Y. Pan, J. Guo, Co-precipitation synthesis route to yttrium aluminum garnet (YAG) transparent ceramics, Journal of the European Ceramic Society 32 (2012) 2971–2979.
[14] J. Li, Y. Pan, F. Qiu, Y. Wu, J. Guo, Nanostructured Nd:YAG powders via gel combustion: the influence of citrate-to-nitrate ratio, Ceramics International 34 (2008) 141–149.
[15] D. Chen, E.H. Jordan, M. Gell, Sol–gel combustion synthesis of nanocrystalline YAG powder from metal-organic precursors, Journal of the American Ceramic Society 91 (2008) 2759–2762.
[16] M.K. Cinibulk, Synthesis of yttrium aluminum garnet from a mixed-metal citrate precursor, Journal of the American Ceramic Society 83 (2000) 1276–1278.
[17] Q. Lu, W. Dong, H. Wang, X. Wang, A novel way to synthesize yttrium aluminum garnet from metal–inorganic precursors, Journal of the American Ceramic Society 85 (2002) 490–492.
[18] Y.H. Zhou, J. Lin, M. Yu, S.M. Han, S.B. Wang, H.J. Zhang, Morphology control and luminescence properties of YAG:Eu phosphors prepared by spray pyrolysis, Materials Research Bulletin 38 (2003) 1289–1299.
[19] X. Li, H. Liu, J. Wang, H. Cui, F. Han, R.I. Boughton, Production of nanosized YAG powders with spherical morphology and nonaggregation via a solvothermal method, Journal of the American Ceramic Society 87 (2004) 2288–2290.
[20] X. Zhang, H. Liu, W. He, J. Wang, X. Li, R.I. Boughton, Synthesis of monodisperse and spherical YAG nanopowder by a mixed solvothermal method, Journal of Alloys and Compounds 372 (2004) 300–303.
[21] M. Zarzecka, M.M. Bućko, J. Brzezińska-Miecznik, K. Haberko, YAG powder synthesis by the modified citrate process, Journal of the European Ceramic Society 27 (2007) 593–597.
[22] P. Palmero, C. Esnouf, L. Montanaro, G. Fantozzi, Influence of the co-precipitation temperature on phase evolution in yttrium–aluminium oxide materials, Journal of the European Ceramic Society 25 (2005) 1565–1573.
[23] H. Wang, L. Gao, K. Niihara, Synthesis of nanoscaled yttrium aluminum garnet powder by the co-precipitation method, Materials Science and Engineering: A 288 (2000) 1–4.
[24] J. Su, Q.L. Zhang, C.J. Gu, D.L. Sun, Z.B. Wang, H.L. Qiu, A.H. Wang, S.T. Yin, Preparation and characterization of $Y_3Al_5O_{12}$ (YAG) nano-powder by co-precipitation method, Materials Research Bulletin 40 (2005) 1279–1285.
[25] I.-W. Chen, X.-H. Wang, Sintering dense nanocrystalline ceramics without final-stage grain growth, Nature 404 (2000) 168–171.
[26] Z.-H. Chen, J.-T. Li, J.-J. Xu, Z.-G. Hu, Fabrication of YAG transparent ceramics by two-step sintering, Ceramics International 34 (2008) 1709–1712.
[27] J. Li, Y. Ye, Densification and grain growth of Al_2O_3 nanoceramics during pressureless sintering, Journal of the American Ceramic Society 89 (2006) 139–143.